

# Multi-angle Imaging SpectroRadiometer (MISR) design issues influenced by performance requirements

Carol J. Bruegge, Mary L. White, Nadine C.L. Chrien,  
Enrique B. Villegas, and Nasrat Raouf  
*Jet Propulsion Laboratory, California Institute of Technology*  
4800 Oak Grove Dr., Pasadena, Ca. 91109

## ABSTRACT

- The design of an Earth remote sensing sensor, such as the Multi-angle Imaging SpectroRadiometer (MISR), begins with a set of science requirements and is quickly followed by a set of instrument specifications. It is required that the sensor meet these specifications across the image field, over a range of sensor operating temperatures, and throughout mission life. In addition, data quality must be maintained irrespective of bright objects, such as clouds, within the scene, or out-of-field glint sources. During the design phase of MISR, many refinements to the conceptual design have been made to insure that these performance criteria are met. These design considerations are the focus of this paper. Spectral stability with field angle, scene polarization insensitivity, and UV exposure hardness have, for example, been enabled through a telecentric optical design, a gaussian shaped filter spectral profile used in conjunction with a Lyot depolarizer, and contamination prevention through considerations in material choices and handling procedures. Spectral, radiometric, and MTF stability of the instrument assures the scientific community that MISR imagery can be used in aerosol, hi-directional reflectance distribution function (BRDF), and cloud studies without constant review of the instrument's health and operating conditions during data acquisition.

## 1. INTRODUCTION

The Multi-angle Imaging SpectroRadiometer (MISR) has calibration and performance requirements which are challenging as compared to those specified for previous generation remote sensing systems. The instrument is to measure incoming spectral radiance to within 3% in absolute units of energy. (MISR will be calibrated to Système International standards<sup>1</sup>, or "SI" units, which are those adopted and recommended by the Eleventh General Conference on Weights and Measures held 11-20 October 1960 in Paris, France.) To accomplish this calibration a comprehensive set of tools are to be utilized, including detector-based radiometric standards, an on-board calibration system which illuminates the entire camera geometric and stray-light fields-of-view, and plans to acquire surface and atmospheric data during an "overflight calibration". The latter uses a computation of incident radiance, using the field measurements or aircraft underflight data, and provides a calibration independent of that determined preflight or by using the on-board calibrator. This reduces calibration uncertainty, as systematic errors present in each technique are averaged out.

Calibration activities, like those described above, are those conducted to derive quantitative descriptors of the instrument features, and are needed within MISR data processing algorithms. Thus, the radiometric, spectral, camera pointing directions, and camera fields-of-view are measured at the end of the camera development phase. Such attention to sensor calibration would be pointless, however, if the instrument suffered temporal instabilities, image history effects such as memory of bright objects, or stray-light contamination of a scene under study. For this reason many design features are incorporated into MISR to insure instrument performance over the anticipated range of sensor operating conditions and scene types. They come to the attention of the design engineer through the instrument science specifications<sup>2</sup>, and are verified either by test or analyses before instrument delivery to the spacecraft integrator. Such an instrument characterization is needed to give assurance to the data user that the MISR data products are valid to within the stated uncertainties, irrespective of pixel position within the sensor, sensor operating temperature, time since launch, or nature of the scene under evaluation. A select number of these design features are reviewed here, in greater depth than that covered in the MISR instrument overview paper presented previously<sup>3</sup>.

## 2. INSTRUMENT STABILITY

### 2.1 Contamination

**MISR** is required to **maintain** a 0.5% radiometric stability during a month, and 2% per year. These values are **needed** to that calibration coefficients applied as a result of one study are appropriate to data sets acquired at different points in time. If care is not taken, the effects of contamination could be the biggest potential source of instrument instability. Of particular concern are the photoactive chemical species which may collect on the camera optical elements, and which may brown and become opaque upon exposure to *W* irradiation. During the course of an orbit, the MISR C and D camera front elements are directly illuminated by **sunlight**, for a period of about four minutes per orbit. Figure 1 depicts this situation, for the D-aft camera, the camera for which **the** illuminated area is greatest in extent. In addition, each time the calibration panels are deployed, **all** cameras are exposed to *W* *reflected* sunlight. The accumulative exposure **to** this latter energy source is about 100 hours over the mission life.

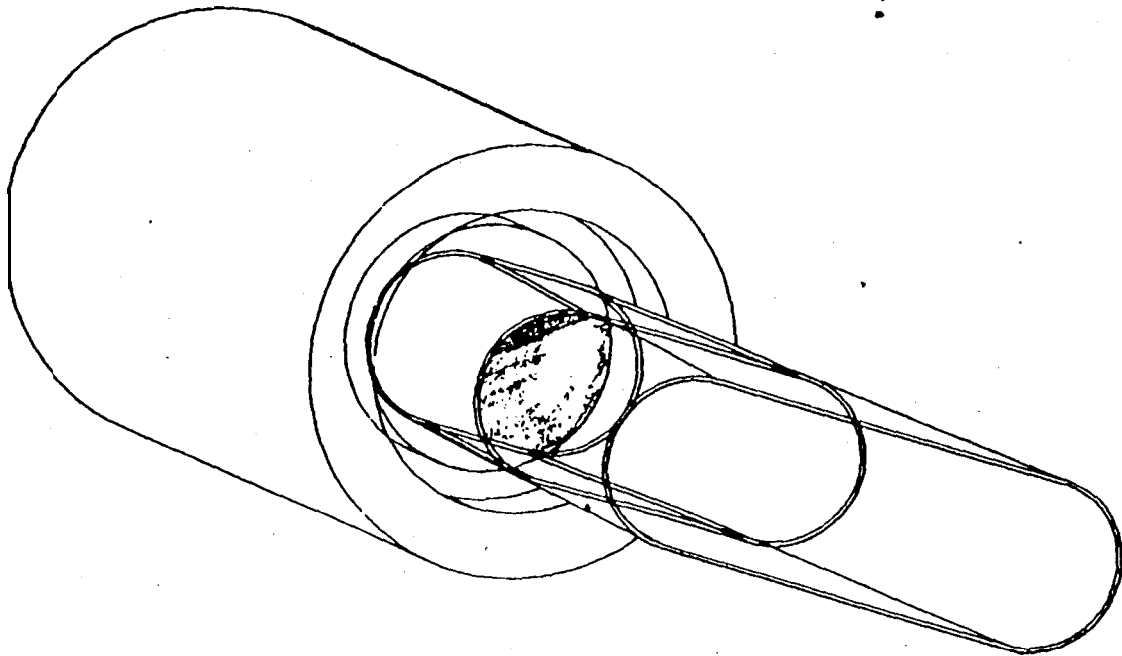


Figure 1. Fraction of front element exposed to *W* illumination during polar region passage. Shown is worst-case **D-aftward** looking camera.

**Because** of the potential for contamination-induced degradation of the optical throughput, the MISR team is taking great care to insure the instrument is contamination free. External surfaces are manufactured such that they are cleanable, with ethanol alcohol, or by some surface-specific cleaning technique. Materials used for the instrument must be approved by the materials engineer and must be **free** from the potential to crack or produce particles, be minimal] y outgassing, and are designed to withstand thermal **bakeout** procedures.

An additional self-protection measure is the plan to keep MISR under a positive pressure flow of gas from a liquid nitrogen tank. The gas is filtered and dried to military and **JPL** specifications, and the instrument is designed to withstand 200% of this gas pressure without damage. Venting of the effluents will be away from the contamination sensitive surfaces.

The accumulation of particulate and molecular contaminants must be controlled **to** the extent that an insignificant change in optical, throughput results. The effects of accumulation of contaminants due to **thrust** exhaust plumes must also be considered. Analyses to date has demonstrated that this effect will be small. The propellant used by the spacecraft will never be directed into the MISR **line-of-sight**, except through **re-emission** from other surfaces. Calculations show that this **re-emission** rate is small, As an added

precaution, however, MISR will be equipped with an instrument cover which can be deployed should this be determined necessary at some later date.

## 2.2 Environmental exposure

Another area of study relevant to camera stability is the effect of the in-orbit environment. In general, **electron** and proton particulate, and **UV irradiance** are known to induce transmission changes in optical glass. **Specifically**, ionization can **occur** when energy sufficient to overcome the energy gap is provided to an electron within an optical **glass**. This freed electron can, in turn, create a defect center with increased absorption. Likewise, these environmental elements can create damage centers in photodetectors. The effects of atomic oxygen also have to be addressed. For many of the components **used** within **MISR**, there is **no** previous performance data relevant to our particular mission dosage levels. Indeed, there is no flight data at all on **Spectralon**, **used** as the MISR calibration **target**.

The stability of several candidate MISR **glasses** has now been tested in an environment simulating electron and proton exposure levels throughout the EOS mission<sup>4</sup> From these tests it has been **determined** that there is no need to be limited to cerium-doped, radiation resistant glasses. The detectors used within the MISR focal plane have likewise undergone radiation testing. It is found that there is an increase in dark current with exposure, but that the MISR signal-to-noise requirements are still met, even assuming end-of-life dark current values. Finally, simulations of the proton environment and its impact of **Spectralon** have eliminated particle radiation as a source of concerns. (Protons are **believed** to be more damaging than electrons, so electron testing was not conducted.)

Atomic oxygen exposure is not believed to be a problem for the MISR instrument<sup>6</sup>. The only optical surface exposed directly to the ram spacecraft direction is the North pole calibration **plate**, that is the forward plate which swings aftward over the North **pole** to enable calibration of the aftward viewing and nadir cameras. The worst case atomic oxygen erosion depth has been calculated to be 6 nm, over the 100 hours of panel use. As the peak-to-valley depth of **Spectralon** is naturally 30  $\mu\text{m}$  or more, the erosion depth is less than 0.02%. It is not expected that this small amount of erosion will effect the optical properties of **Spectralon**.

With these studies, and others planned in the near future, we can verify that the MISR design is robust against the effects of the in-orbit environment.

## 2.3 Filter design

The degradation of camera throughput, as created by contamination and environmental exposure effects can be corrected for with **time**, provided that the instrument eventually becomes stable, and provided the system SNR requirements can still be met. If these criteria are **met**, then a new **radiometric** calibration can be established, in-flight, and the science needs can be met. The problems created by undetected spectral shifts, however, are of a different nature. Without knowing the new bandpass profile it is impossible to restore the instrument calibration to the same level of accuracy as that provided in the absence of any spectral shifts. There has been much published in the literature, for example, on spectral shifts noted during the Landsat program<sup>7</sup> On the Thematic Mapper **(TM)** there were observed shifts in **radiometric** sensitivity measured in going in and out of vacuum in prelaunch tests. These "vacuum shifts" were believed related to the spectral filters. Similar changes were noted shortly after launch. More recently engineers have measured the transmission of witness samples of the TM filters used on **Landsats** 4-6 in and out of vacuum, and have observed bandwidth changes on the order of 5 nm. **These** shifts could account for the observed vacuum shifts. **Landsat-7** will use the newer filter technology.

Prior to the 1980's coatings were used which lacked resistance to moisture and the effects of handling. Currently some of **the** best filters made for narrow-band applications, and requiring stability over time, rely on ion assisted deposition (IAD). (Not all interference layer materials are **inherently** instable, so it would be misleading to infer a given filter is necessarily instable without this technology.) In this process an ion source is utilized during plasma deposition of the oxide coatings. This allows for compactness in the layer coating, and this in turn **precludes** the layer from **the** adverse consequences of moisture **absorptance**. As **well as** packing density, adherence and other factors are improved. The durability of filters produced using IAD technology has

been demonstrated as they have been cycled to 300°C, and submersed in liquid nitrogen, without detectable effects. Other examples of IAD stability tests follow.

In 1988 BARR Associates produced for the Research in Astronomy (AURA) in Tucson, Arizona an IAD filter of 8 Å width and 679 nm center wavelength. **Three** other filters were produced at the same time. AURA devised a test consisting of temperature cycling from 26 to 46°C and **back**, seven times daily. After three years of testing the conventional filters had shifted by 2-3 Å, and the IAD filter had not shifted to within 1 Å uncertainty.

Other in-house testing at BARR has verified wavelength stability. A 340 nm filter with an 8 nm bandpass had been made with the Ta<sub>2</sub>O<sub>5</sub> IAD process. After 5300 hours of exposure at 95% RH and 65°C, the center wavelength was found to be stable, to within 0.-15 nm measurement uncertainty, as was the **FWHM** stayed the same (to 0.01 nm uncertainty). The measurements were taken with **a** Cary 2400 with an assumed wavelength **error** of **±0.1** nm.

### 3. SPECTRAL UNIFORMITY

#### 3.1 Telecentric optical design

There are many design objectives which have driven the **MISR optical** layout. It is desirable, for example, to minimize the number of optical elements, as well as the weight and volume of **the** lens. Materials must be selected which are stable in the on-orbit environment. In addition, there are many image fidelity requirements. These include acceptable image distortion and MTF, relative illumination uniformity across the focal plane for a uniform **input**, and **athermalization** to assure focus and a constant **focal** length with temperature. The requirement to accept only slight deviations in center wavelength and bandpass along an array is made, however, not to assure image fidelity, but rather data product fidelity. That is, without this requirement the departure in these parameters from on-axis values could yet be determined through **modelling** and calibration. Each image pixel would therefore provide an equally accurate measure of the scene radiance with which it observes. Here, however, the wavelength at which the radiance is reported would vary along the cross-track image swath. The science user would inherit an excessive data interpretation problem. It would not be clear if differences in retrieved reflectance were a result of spatial, or spectral scene reflectance differences.

The MISR **spectral** specifications include a requirement to permit no more than a **±2.0** nm shift in central wavelength or deviation in bandwidth across the array, for the 0.865 nm worst case band. (The allowable shift in center bandwidth is **±1.0** nm for Bands 1 and 2, and **±1.5** nm for Band 3.) These requirements were not initially met in the original MISR optical layout. Here a Double Gauss configuration was chosen, a six element design which is a powerful lens design format featuring good distortion control including low chromatic and spherical **aberrations**. The main difficulty with this traditional telescope design was its inability to meet the wavelength uniformity specification. The design was estimated to produce a 2 to 4 nm shift across the focal plane, for Bands 1 and 4 respectively. The current design, shown in Figure 2 for one of the four MISR camera designs, is nearly **telecentric** in image space. There is only a 3° shift in the cone angle of illumination, as compared to that for on-axis illumination. The **design** is achieved through use of an added seventh element which images the exit pupil at infinity.

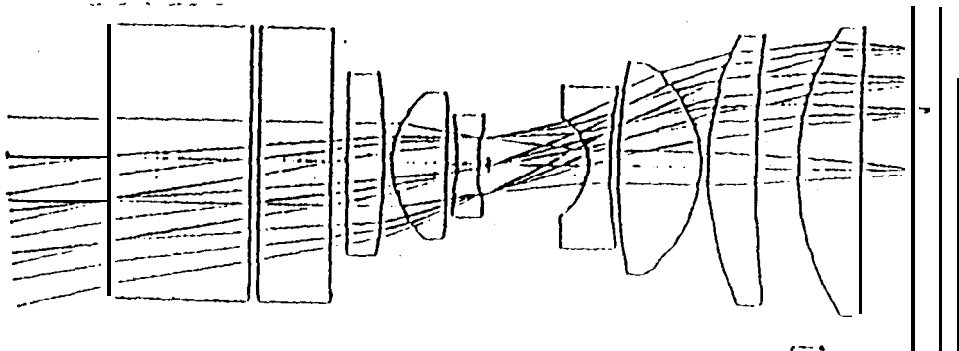


Figure 2. Telecentric optical design for Camera A design

The undesirable spectral shift in **the** original optics design was a result of varying incidence angle across the **filter** interference coatings. For interference filters in general there is a **shift** toward shorter wavelengths with increasing angle of incident of the impinging light. The magnitude of this effect is related to the effective index of the multi-layer coating. This index lies between the refractive indices of coating materials. For a given design, the effective wavelength shift is a **function** of the light cone used during imaging. The result for the **MISR** F/5.5 system is shown in Figure 3, solid line. The dashed line represents the **spectral** shift due to the 3° shift across the focal plane. It is found that the shift is 0.35 nm. This effect is seen as a wavelength shift with position on the focal plane, and is well within the **MISR** science specification. **This** analyses was done separately on the blocking-layers, those layers deposited so as to allow the out-of-band spectral light **leaks** to be controlled. Almost no change was noted for these layers alone.

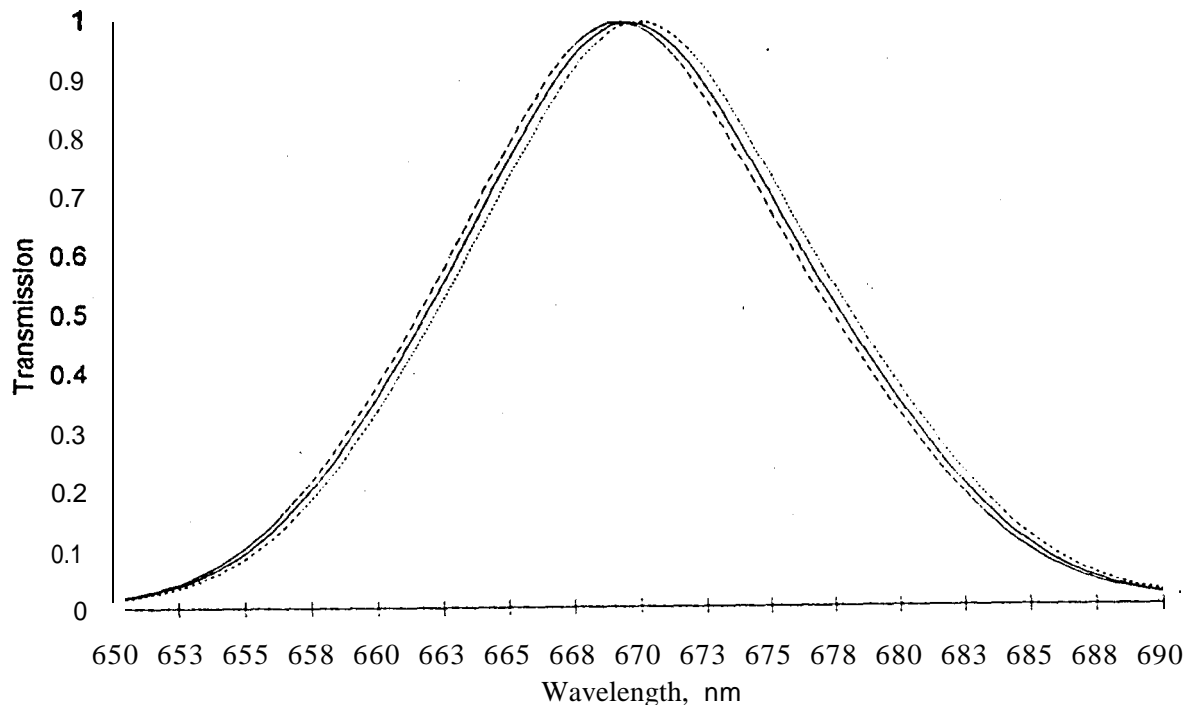


Figure 3. predicted **filter** spectral throughput for **MISR** F/5.5 system. Solid line in is filter output as viewed by an on-axis pixel, dashed line is edge-of-field response.

Other sources of filter nonuniformities across the array are due to the manufacturing process. There are a number of process-related factors that can effect the uniformity. Among them are geometrical configuration of the parts during deposition and thermal gradients across a part during deposition. Both of these are affected by tooling, heating techniques, mounting techniques, photolithography stencils, and others. With current control capability, the uniformity can be controlled to within 0.5 nm across the array, and to within 0.75 nm between filters. Another insignificant contributor to spectral shifts is the effects of temperature. Commonly used films suffer from changes in refractive index and layer thickness, which in turn changes the optical path length. This typically causes a shift toward shorter wavelengths with a decrease in temperatures. **With IAD oxides the temperature** coefficient is less than 0.005 nm per degree C. This is a factor of five less than traditional coatings. Temperature induced spectral shifts are therefore believed not to be a problem for **MISR**. The geometric effect of wavelength shift with angle is found to be the only significant contributor to spectral **nonuniformity** either across the filter, or from one filter to another.

#### 4. RADIOMETRIC ACCURACY

##### 4.1 Contrasting targets

The **MISR** science team is interested in the effects of the **optical** point-spread function (**PSF**) on the **radiometric** accuracy and frequency response of each camera design. The **PSF** includes the effects of diffraction, optical aberrations, scattered light, charge diffusion within the CCD, and CCD charge transfer inefficiency. (Scattered light is **defined** here as that which originates from

sources within the camera field-of-view.) In order to verify radiometry accuracy in the presence of these effects, the MISR instrument requirements have defined two scenes which typifies situations believed to be problematic. The first scene consists of two half-planes of **5%** and **100%** reflectance. The radiance on the dark side is specified to be accurate to within **2%**, at a point 24 pixels from the boundary. The second scene consists of a 5% reflecting region, 24x24 pixels in size, surrounded by a 50% reflecting background. The retrieved radiance for any pixel within the dark region, is specified to be no more than 2% of the radiance measured in the absence of the background. It is noted that the instrument requirements do not specify that the **radiometric** accuracy must be achieved through instrument 'design only. It is undetermined at this point if MISR will construct algorithms to correct for PSF over **contrasty** scenes, It is **likely** that if this **technique** is developed, however, it may only be applied to a limited number of scenes of particular interest to the science community.

The above specifications dictate that the MISR engineering staff put considerable effort into characterizing the **radiometric** accuracy – **for** these two scene types, The approach actually to be used, however, is to model the PSF at various points both within and out-of the camera geometric field-of-view. This latter approach is preferred, in that this information can be used to predict the **radiometric** accuracy for any scene contrast. To accomplish this task many math models will be used, The optical design code will model the predicted PSF due to diffraction and **optical** aberrations. These results are combined with those from a scatter-analyses code, and the degradations expected due to detector effects. These data are used to construct the system response to the contrasting scenes **described** above.

A limited amount of testing will **also** be done to verify the above model **analyses**. That is, the system PSF will be characterized at a limited number of **field** positions. This will **confirm** the model PSF computed as described above. Although it will not be possible to actually construct a target to represent to two scenes described above, a **close** representation will be provided. The **modelling** effort will then predict the **radiometric** error for this test target, thus allowing a comparison of model and actual test data.

#### 4.2 Stray light

It is required that stray light from out-of-field sources be rejected such that the **radiometric** accuracy is **preserved** for a scene under study, To accomplish this task MISR has made use of a stray-light code, and **modelled** the PSF for out-of-field sources, This activity has led to some design changes within the camera. The out-of-field PSFS will again be computed for the new design, thus estimating the stray-light effects for our final system.

The above model analyses will **be** verified using point sources to 5° outside the camera FOV. Because of constraints imposed by our **thermal** vacuum chamber, this is the limit of the test. The engineering team, therefore, is making full use of analyses to verify the instrument requirements.

#### 4.3 Polarized incident radiance

The accuracy with which **MISR** measures an incident radiance field must be maintained, **irrespective** of the incoming state of **polarization**. This is not necessarily guaranteed for a system, as the amount of light reflected at each optical interface depends on this state. This effect is described by the **Fresnel** reflection coefficients, and results in a **polarization** dependent transmittance for the system. It is not possible **to** calibrate the sensor for this effect, as the scene **polarization** properties are not **simultaneously** measured or otherwise known,

The MISR polarization requirement implies that the **detector output**, resulting from a stimulus of arbitrary plane of **polarization**, shall not deviate by more than **2%** over that measured while viewing an unpolarized stimulus. This allowable error is a **sizeable** portion of the total **radiometric** error budget of **3%**. *The* MISR conceptual optics design, however, did not meet this specification. In this design a single layer MgF<sub>2</sub> anti-reflection coating layer was assumed, The layer increased transmission and **decreased diattenuation**. **Diattenuation** is defined as  $D = (T_p - T_s) / (T_p + T_s)$ , and describes the maximum dependence of system transmittance on the incident **polarization** state. Here  $T_p$  and  $T_s$  are the transmission coefficients for p and s polarized light (light polarized parallel and perpendicular to the plane of incidence). For an ideal system  $D=0$ .

The current design replaces the single layer  $\text{MgF}_2$  anti-reflection layer with a six element stack. With this the lens **diattenuation** decreases from 20% to 3% at the worst case wavelength and field angle. More significant, however, is the performance improvement gained through use of a Lyot **depolarizer**. This added optical element is used in conjunction with a gaussian **spectral** band shape, hence the MISR requirement of a gaussian filter design. For ideal performance the system response would be **gaussian** in frequency, not wavelength. It has been determined, however, that requiring the filter to be roughly gaussian in wavelength is sufficient. The **transmittance** of an individual filter will approximately correspond to  $\tau_{g,\lambda} = \tau_g \exp(-((4 \ln 2) (\lambda - \lambda_{c,g})^2 / (\Delta\lambda_g)^2))$ , where  $\tau_g$  is the peak transmittance,  $\lambda_{c,g}$  the wavelength at peak transmittance, and  $\Delta\lambda_g$  the full width half maximum (FWHM) of the band.

A Lyot depolarizer consists of two birefringent plates rotated by  $45^\circ$  relative to each other. The Lyot depolarizer to be used by MISR will be composed of  $\text{MgF}_2$ , which has a high birefringence, and will be approximately 1", for the camera A design, and 1/2" long for the D-design. The added thickness of the crystal needed for the nadir camera is a result of the larger field angles covered by this lens, and **greater diattenuation**. The two elements are separated by an air gap, rather than optically contacted. Thermal gradients may separate optically contacted elements, resulting in destructive interference effects. These plates introduce a large **retardance** variation across the spectral band of the instrument **effectively** depolarizing the incident light. The ability of a Lyot to provide an unpolarized emerging **field** is dependent on the "degree of coherence" of the spectral band in question. This is basically a Fourier transform of the incoming **spectral** signal, and is not monotonic for the conventional square-band shape. Other disadvantages of using a square-band profile with the depolarizer is the increased sensitivity to **temperature**, the birefringence being a function of temperature.

With the Lyot, a 100% linearly **polarized** beam would be scrambled to yield an exiting field of 5% polarization, including **Fresnel** losses at the front surface. Allowing for a 5% **diattenuation** of the lens system, and a worst case filter **diattenuation** of 10%, the **radiometric** error of the system is predicted to be 0.5%. It is noted that the filter need not be highly non-polarizing, as the detector is the only remaining component, and it is polarization insensitive.

In reality, very few scenes will be 100% polarized. This could happen, for example, while viewing an ocean **scene**, on a clear (aerosol) free day. The **radiometric** accuracy requirement, therefore, is now thought to be easily achieved. It is also required that a relative **radiometric** accuracy of 0.5% be achieved using a single camera and color channel. As it is unlikely that a scene will be composed of elements which differ by  $90^\circ$  in polarization, this criteria will be met at the  $1\sigma$  confidence level.

#### 4.4 Cloud and bright target saturation

Many of the performance specifications placed upon the MISR instrument require attention to design details within the detector and electronics subsystems. Several problems associated with Landsat-4 and -5 related to electronics are discussed in Kieffer et al.<sup>9</sup>. These included unequal population of digital bins due to non-uniform widths of successive voltage increments in the **analog-to-digital converter (ADC)**, scan-direction dependent level shifts, overshoot at high contrast boundaries, an offset after scan of a bright image that lasted up to 800 pixels, and high-frequency noise. It is the attempt of the MISR design team to avoid these undesirable features in the design, and verify the instrument performance in the verification phase of the instrument build.

The MISR CCD will be designed and fabricated based upon standard 3-phase, **3-poly**, n-buried channel, silicon detector **technology**. The CCD will consist of four independent line arrays each with its separate electronic shutter and output amplifier. A schematic of the CCD architecture, in cross section, is presented in Figure 5. This drawings can be referred to in the description of blooming and saturation control. These undesirable effects may be created if a **large** signal, such as that from an ocean glint or bright cloud, were to be viewed.

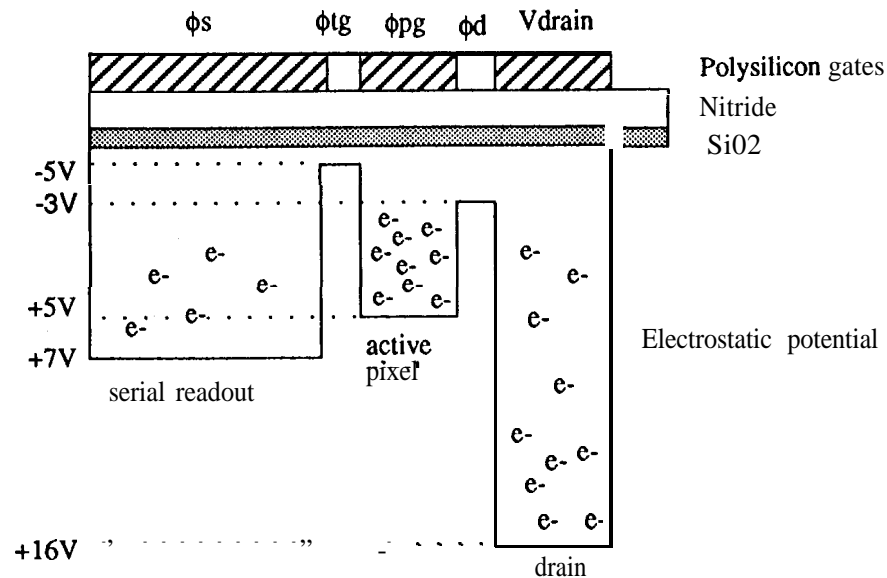


Figure 4. Detector biasing during charge integration.

The process of signal detection and collection begins when the transfer gate,  $\phi_{tg}$ , and dump gate,  $\phi_d$ , are biased low. Here a potential well is created under the photogate region,  $\phi_{pg}$ , which is biased high. The  $\phi_{tg}$  and  $\phi_d$  regions act as barriers which prevent charge from spilling into the surrounding regions. If the capacity of the active pixel region is exceeded, blooming is prevented in the serial direction by the selective biasing of  $\phi_{tg}$  and  $\phi_d$  (to  $\sim -5V$  and  $-3V$  respectively), that is  $\phi_{tg}$  is set more negative than  $\phi_d$ . Once the active pixel is filled, spillage will flow towards the drain region,  $V_{drain}$ , and not into the serial readout registers  $\phi_{s2}$  and  $\phi_{s3}$ . Saturation would only occur if both the active pixel and drain were filled. In the lateral direction, between pixels, the charge is confined by channel stops constructed from thick field oxide.

The capacity for blooming and saturation control was designed to absorb signals of at least  $10^5$  times fullwell without saturating the device. It is noted that large signals may be encountered if a direct specular solar reflection, such as that due to ocean glint, is observed. Such an intensity would be tens of thousands of times greater than that observed by a bright but perfectly diffuse region of a scene. This design has been verified by testing of a prototype detector. It is expected that if the serial register does saturate, that the region will return to the normal dark current level within one or two line times. In addition, the electronic signal chain is equipped with a clamping circuit, to prevent any signal extremes from incurring damage to the back-end electronics.

The MISR instrument specifications state that if blooming occurs due to a signal between one and ten times the detector full well, that pixels at a distance  $\geq 8$  pixels shall be unaffected. This limits the undesirable effect no greater in size than eight unaveraged pixels. Design and testing efforts to date suggest that this requirement will be easily achieved.

#### 4.5 Electronic signal chain

A brassboard assembly of the MISR A-camera design, including focal plane and signal chain electronics has been complete. Through test of this early prototype, the MISR team has begun to verify that the flight camera electronics design is achieving its performance specifications.

The CCD pixel data are clocked out in serial fashion, and fed into a preamplifier which lowers the impedance and acts as a buffer. This signal is fed into a signal chain which uses a "coherent double sampling" technique to control noise. Basically, as the CCD signal is read, a sampling circuit is used which measures the difference between signal and ground. Synchronous sampling is key



to reducing noise between this read and that of the clock signals. CCD white noise is also filtered at this position. From here the signal is sent into the analog to digital converter (ADC). MISR will use a 14 bit ADC. The least significant bit of an ADC is known to have a noise uncertainty of 0.3 bits. By truncating the signal to 13 significant bits, MISR avoids this source of ADC error.

One source of noise within the electronics chain is the Constantine wire used for the ground return. This material was selected for its thermal properties, and has a higher impedance than other materials. These wires must be kept short to minimize noise within the system. All totaled, the noise allocation from these sources is expected to be about 40 electrons. This is insignificant as compared to our ADC sampling interval.

The predicted sources of noise for a MISR camera are depicted in Figure 5. Shown are both the components of noise and total noise,  $N_t$ , as a function of equivalent reflectance,  $p$ , for Band 1 of an A camera. Noise differences between camera design and spectral channel are insignificant. The limiting noise is found to be photon (shot) noise,  $N_p$ , although electronic noise,  $N_e$ , is non-negligible at low reflectance. Due to square-root encoding, the quantization noise,  $N_q$ , does not become a limiting noise factor. The instrument science requirements state that the SNR to be achieved is 700, 600, 450, 300, 100, and "best possible" at equivalent reflectance values of 1., 0.7, 0.5, 0.2, 0.02, and 0.01, respectively. (To translate the SNR requirement vs. equivalent reflectance into SNR vs. radiance, an overhead exo-atmospheric sun is assumed which illuminated a perfectly diffuse panel, at the stated reflectance value.)

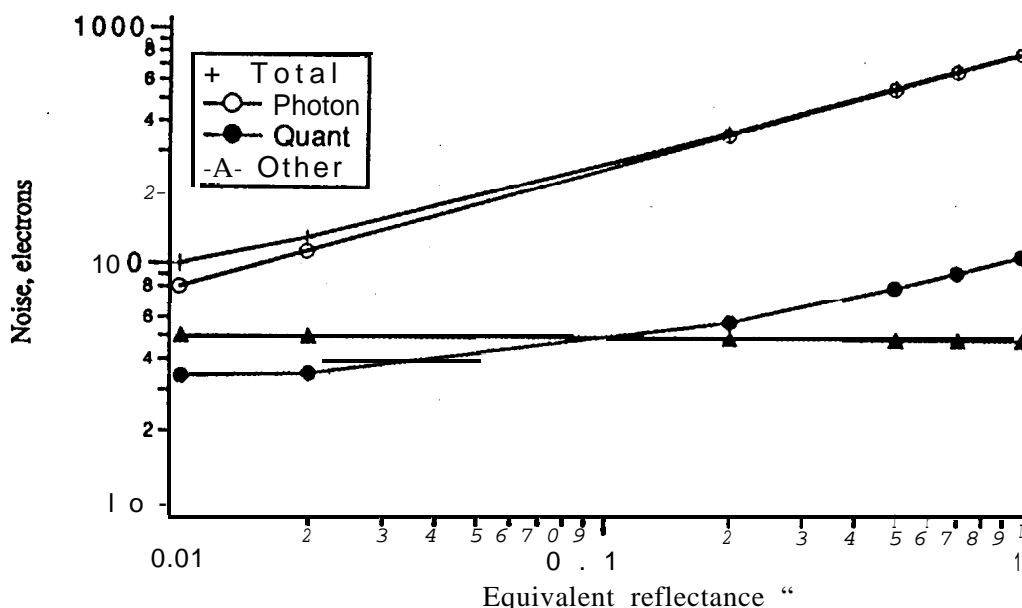


Figure 5. Noise sources for MISR camera.

## 5. CONCLUSIONS

The MISR instrument performance specifications have been produced to assure the data user and scientific community that MISR will provide high fidelity data sets even under adverse conditions such as high contrast scenes and varying input states of polarization. It is believed at this point in time that MISR will achieve these performance requirements. In addition to the build of the engineering model, and following flight hardware, the MISR team is currently involved in detailed planning of the verification test phase of the program.

## 6. ACKNOWLEDGEMENTS

We wish to thank all the members of the MISR design team for their contributions towards the instrument definition and the material presented in this paper. These include David Diner, principal investigator, Elmer Floyd, instrument manager, Larry Hovland,

instrument engineer, Daniel Preston, filter specifications and testing, Richard Rainen, materials selection, Daniel Taylor, Glenn Aveni, and David **Guarino**, contamination. A special thanks is extended to Frank Woodbury and his colleagues at BARR Associates, for providing the material used within the **filter** discussion. The research described in this paper was carried out by the Jet Propulsion Laboratory, California Institute of Technology, under contract with the National Aeronautics and Space Administration.

## 7. REFERENCES

1. **Meyer-Arendt J.R.**, "Radiometry and photometry: units and conversion **factors**," *Appl. Opt.* 7,2081-2084 (1968).
2. Diner, **D.J.** *Instrument Science Requirements*. Jet Propulsion Laboratory document number JPL D-9090 (Revision: February 1993).
3. Diner, **D.J.**, **C.J. Bruegge**, T. Deslis, V.G. Ford, L.E. Hovland, DJ. Preston, **M.J. Shterenberg**, **E.B. Villegas**, and **M.L. White**, "Development status of the EOS Multi-angle Imaging **SpectroRadiometer (MISR)**," in *Sensor Systems for the Early Earth Observing System Platforms*, *Proc. SPIE* 1939 (April 1993).
4. **Al-Jumaily**, G.A., "Effects of radiation on the optical properties of glass **materials**," in *Damage to Space Optics and Properties and Characteristics of Optical Glass*, *Proc. SPIE* 1761,26-34 (July 1992).
5. **Bruegge C.J.**, **A.E. Stiegman**, **R.A. Rainen**, and **A.W. Springsteen**, "Use of **Spectralon** as a diffuse reflectance standard for in-flight calibration of Earth-orbiting **sensors**," *Opt. Eng.*, (April 1992).
6. Lewis, D.F., "Surface morphology and atomic oxygen erosion of **Spectralon**," JPL internal memorandum number **MISR-DFM#160** (1993),
7. Barker, J.L., **R.B. Abrams**, **D.L. Ball**, and **K.C. Leung** in *Landsat-4 Science Characterization Early Results*, NASA CP-2355, 11373-474 (1985).
8. McGuire, **J.P.** "Feasibility of Lyot **depolarizers** for **MISR**," JPL internal memorandum number **MISR-DFM#58** (June 1991).
9. Kieffer, H.H., D.A. Cook, **E.M. Eliason**, and **P.T. Eliason**, "Intraband radiometric performance of the Landsat Thematic Mappers," *Photogramm. Eng. and Remote Sens.* 51,1331-1350 (1985).